

Field-Induced Fluorescence Quenching and Enhancement of Porphyrin Sensitizers on TiO₂ Films and in PMMA Films

Hung-Yu Hsu,[†] Hung-Chu Chiang,[‡] Jyun-Yu Hu,[†] Kamlesh Awasthi,[‡] Chi-Lun Mai,[§] Chen-Yu Yeh,^{*,§} Nobuhiro Ohta,^{*,‡} and Eric Wei-Guang Diau^{*,†}

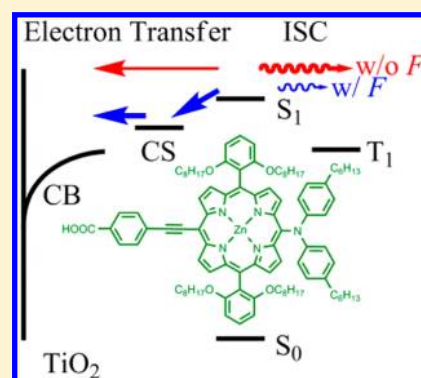
[†]Department of Applied Chemistry and Institute of Molecular Science, National Chiao Tung University, Hsinchu 30010, Taiwan

[‡]Research Institute of Electronic Science, Hokkaido University, Sapporo, Japan

[§]Department of Chemistry and Center of Nanoscience & Nanotechnology, National Chung Hsing University, Taichung 402, Taiwan

Supporting Information

ABSTRACT: Three highly efficient porphyrin sensitizers—YD2, YD2-oC8, and YD30, either sensitized on TiO₂ films or embedded in PMMA films—were investigated using electrophotoluminescence (E-PL) spectra. Under both thin-film conditions, on application of an external electric field we observed the quenching of fluorescence of push–pull porphyrins (YD2 and YD2-oC8) and a slightly enhanced fluorescence of the reference porphyrin without an electron donor group (YD30). A nonfluorescent state with charge separation (CS) is proposed to be involved in both YD2 and YD2-oC8 systems so that the electron injection becomes accelerated in the presence of a strong electric field. In contrast, the retardation of the nonradiative process not involving a CS state was the reason for the field-induced enhancement of fluorescence of YD30. The extent of fluorescence quenching of YD2-oC8 was greater than that of YD2 on TiO₂ films, indicating that the *ortho*-substituted long alkoxy chains play a key role to accelerate the consecutive electron injection involving the CS state. Our E-PL results indicate that a field-induced variation of fluorescent intensity is related to the efficiency of conversion of solar energy and that further improvement of the performance of devices containing push–pull porphyrin dyes is achievable under an applied electric field.



1. INTRODUCTION

Dye-sensitized solar cells (DSSC) have attracted much attention because of their potential as next-generation photovoltaic devices.^{1–6} A promising example was shown by a device made of a porphyrin dye (YD2-oC8) in a cobalt electrolyte that attained efficiency 12.3% of power conversion (PCE),⁷ which is superior to devices developed based on Ru complexes^{8,9} or metal-free organic dyes.^{10,11} In general, the aggregation of porphyrins with a large planar π -conjugation is feasible.^{12,13} Our previous work on push–pull porphyrin sensitizers showed that a promising zinc porphyrin (YD2) can effectively diminish dye aggregation and enhance device performance.^{14–16} To suppress further the extent of dye aggregation, YD2-oC8 was designed with long alkoxy chains attached at the *ortho*-positions of the *meso*-phenyls of the porphyrin. These *ortho*-substituted devices outperformed their *para*- and *meta*-substituted counterparts because a substitution of the long alkoxy groups at the *ortho*-position protects the porphyrin cores from dye aggregation and from forming a blocking layer on the TiO₂ surface.^{5,17,18}

Electroabsorption (E-A) and electrophotoluminescence (E-PL) spectra, i.e., plots of the change of an absorption spectrum and photoluminescence spectrum, respectively, induced with an electric field have been extensively used to examine electronic properties, such as electric-dipole moment and molecular

polarizability, for organic and polymeric thin-film systems.^{19–23} Several authors reported the effects of local electric fields on the optical properties of DSSC.^{24–26} Meyer and co-workers assigned the spectral shift of the peak bleach of the metal-to-ligand charge-transfer (MLCT) band to be due to the Stark effect induced by an electric field on the oxidized sensitizers.²⁴ Pastore and Angelis interpreted the observed spectral shift of the peak bleach in photoinduced absorption (PIA) spectra, which show absorption spectra of a sample to differ with and without photoexcitation, to be caused by the Stark effect, based on computational results.²⁵ Boschloo and co-workers reported that the spectral shape of the E-A signals is similar to that of the PIA signals of an organic dye adsorbed on a TiO₂ thin film, which is given by the first derivative of the absorption spectra of the dye.²⁶ The effect of an electric field on absorption and emission spectra has hence some impact on the further understanding of molecular interactions and electron-transfer properties at the dye/TiO₂ interface.

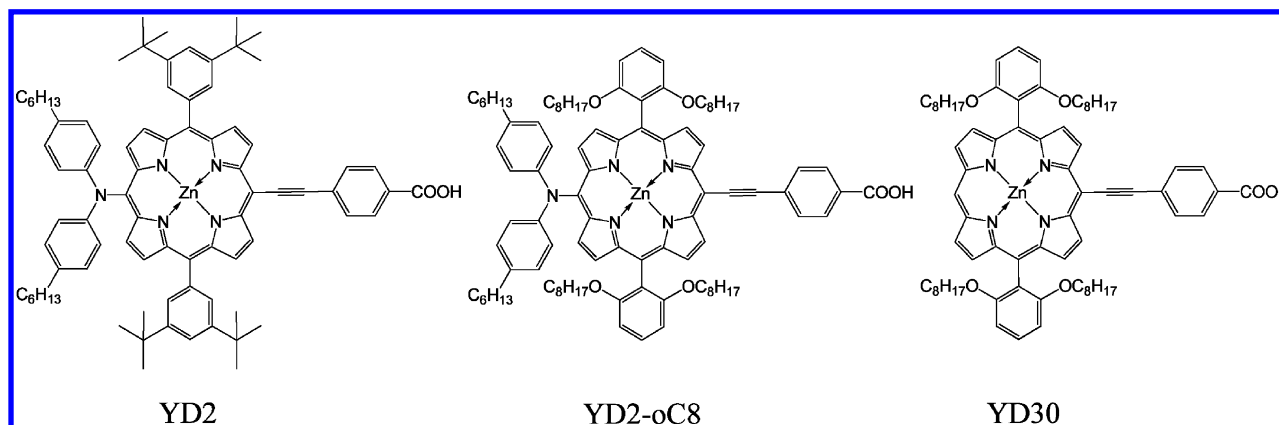
In the present work, we present E-PL spectra of the three porphyrin dyes YD2, YD2-oC8, and YD30 (Scheme 1) embedded in PMMA films or sensitized on TiO₂ films. The

Received: October 4, 2013

Revised: November 7, 2013

Published: November 7, 2013

Scheme 1. Molecular Structures of YD2, YD2-oC8, and YD30



synthetic details of YD2 and YD2-oC8 are reported elsewhere;^{7,14–16} those of YD30 are given in the Supporting Information. We found that the fluorescence of YD2 and YD2-oC8 was quenched on application of an electric field and that the fluorescence of YD30 was slightly enhanced with an electric field. To account for the observed quenching of fluorescence under an applied electric field, we propose that the electron injection in the push–pull porphyrin system involves a state with charge separation (CS).

2. EXPERIMENTAL SECTION

The TiO₂ nanoparticles (NP) were prepared according to a conventional synthetic procedure and then prepared as a paste for screen printing according to a procedure reported elsewhere.²⁷ For the working electrode, the TiO₂ NP as a transparent active layer was coated on a TiCl₄-treated FTO glass substrate (TEC 7, Hartford) to obtain a film of thickness ~3 μm and active size 0.4 × 0.4 cm². The TiO₂ films were then immersed in a solution containing the target porphyrins (YD2, YD2-oC8, or YD30, 1.5 × 10⁻⁴ M) and chenodeoxycholic acid (CDCA, 7.5 × 10⁻⁴ M) in ethanol for 30 min. Then the porphyrin-sensitized TiO₂ films were rinsed by ethanol for several times in order to remove the unadsorbed or weakly bonded dye molecules on the surface of TiO₂. The counter electrode was made on spin-coating the H₂PtCl₆/isopropanol solution onto a FTO glass substrate (FTO, 8 Ω/cm², typical size 1.0 × 1.5 cm²) through thermal decomposition at 380 °C for 30 min. The electrolyte solution containing I₂ (0.05 M), LiI (0.1 M), PMII (1 M), and 4-*tert*-butylpyridine (0.5 M) in a mixture of acetonitrile and valeronitrile (volume ratio = 85:15) was introduced into the space between the two electrodes, completing the fabrication of these DSSC devices.

For the porphyrin:PMMA thin films, the porphyrin embedded in PMMA was deposited on an ITO-coated quartz substrate on spin coating from a toluene solution in which a mixture of porphyrin and PMMA (mass ratio = 1:40) was dissolved. The thickness of the sample was ~0.5 μm, measured with an interferometric microscope (Nano Spec/AFT-010-0180, Nanometric). A semitransparent Al film was further deposited on the sample film with vacuum vapor deposition. For the porphyrin/TiO₂ thin films, the porphyrin adsorbed on transparent TiO₂ layer on FTO glass substrate ~3 μm, and then a PMMA thin film of thickness ~1 μm was deposited on the TiO₂ film as an insulator. There was a further Al film deposited on the PMMA thin film. ITO/FTO and Al films served as electrodes for both samples.

Electric-field-induced changes in fluorescence spectra were measured using electric field modulation spectroscopy described elsewhere.²⁸ Briefly, the electrofluorescence spectra and fluorescence spectra were investigated with a spectrofluorometer (FP777, JASCE) equipped with a modulation apparatus. Electromodulation of fluorescence intensity was induced by a sinusoidal ac voltage with a frequency 40 Hz. A function generator (SG-4311, Iwatsu) combined with a homemade amplifier was used to generate an ac voltage up to 100 V. The external-field-induced fluorescence change was detected with a lock-in amplifier (SR830, SRS) at the second harmonic of the modulation frequency.

The total fluorescence (PL) intensities of the porphyrin dyes would be significantly quenched when they were adsorbed on TiO₂ as compared to that of free dye in PMMA because the interfacial electron transfer is a very efficient nonradiative process to compete with the emission process.²⁹ Therefore, the PL and the corresponding E-PL spectra of the TiO₂ films were recorded under a greater light-collection condition than those of the PMMA films.

3. RESULTS AND DISCUSSION

When an external electric field (F) is applied to a molecule, the molecular energy levels become shifted through the interaction of the permanent electric-dipole moment and the molecular polarizability with F .³⁰ The field-induced spectral shift in energy (ΔE) is expressed by the equation

$$\Delta E = -\Delta\mu F - \frac{1}{2}F\Delta\alpha F \quad (1)$$

in which $\Delta\mu$ and $\Delta\alpha$ represent the differences in electric dipole moment and molecular polarizability, respectively, between two states between which an optical transition occurs. Assuming that the isotropic distribution of absorbers and emitters is maintained at the second harmonic of the modulation frequency of F , the E-PL spectrum in wavenumber, $\Delta I_F(\bar{\nu})$, is expressed as a linear combination of the zeroth, first, and second derivatives of the emission spectrum^{30,31}

$$\Delta I_F(\bar{\nu}) = |fF|^2 \left\{ A I_F(\bar{\nu}) + B \bar{\nu}^3 \frac{d}{d\bar{\nu}} \left[\frac{I_F(\bar{\nu})}{\bar{\nu}^3} \right] + C \bar{\nu}^3 \frac{d^2}{d\bar{\nu}^2} \left[\frac{I_F(\bar{\nu})}{\bar{\nu}^3} \right] \right\} \quad (2)$$

in which coefficients A , B , and C correspond to the field-induced change of fluorescent intensity, the spectral shift mainly resulting from $\Delta\alpha$, and the spectral broadening mainly resulting from $\Delta\mu$, respectively; f is the internal field factor. The magnitude of $\Delta I_F(\bar{\nu})$ is proportional to the square of the strength of the applied field; this relation is clearly shown in Supporting Information Figure S1 for YD2 embedded in PMMA and sensitized on TiO₂. We hence fit the E-PL spectra with a linear combination of the PL spectrum and its first- and second-derivative spectra, as indicated in eq 2. Assuming a random distribution of fluorophores in an immobilized solid film, we express coefficients B and C roughly as

$$B = \frac{\Delta\bar{\alpha}}{2hc}, \quad C = \frac{|\Delta\mu|^2}{6h^2c^2} \quad (3)$$

in which $\Delta\bar{\alpha}$ denotes the average of the trace of $\Delta\alpha$, h is Planck's constant, and c is the speed of light.

For the E-PL spectra reported herein, we employed a thin-film system with TiO₂ films of thickness $\sim 3 \mu\text{m}$ (one single transparent layer of TiO₂ nanoparticles without an added scattering layer) for improved collection of optical signals from the thin-film samples. We tested the performance of devices with these thin TiO₂ films. Figures 1a and 1b show the

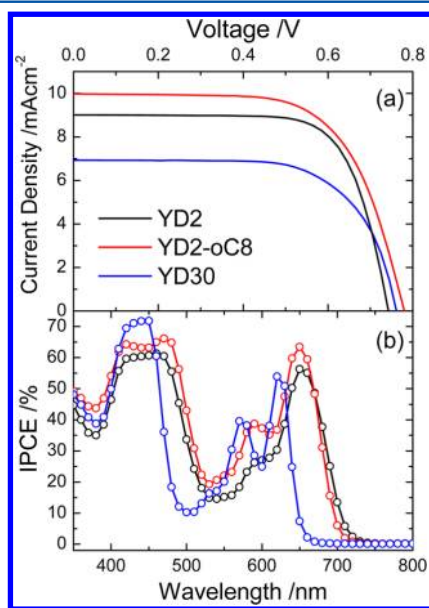


Figure 1. (a) Current–voltage characteristics and (b) corresponding IPCE spectra of solar cells sensitized with YD2 (black traces), YD2-oC8 (red traces), and YD30 (blue traces). The devices were fabricated with working electrodes containing only one single layer of TiO₂ nanoparticles of thickness $\sim 3 \mu\text{m}$.

current–voltage curves and the corresponding spectra of efficiency of conversion of incident photons to current (IPCE) of the devices sensitized with YD2, YD2-oC8, or YD30 in an iodine-based electrolyte; the corresponding photovoltaic parameters are summarized in Table 1. The performances of these devices show a systematic trend on J_{SC} with order YD2-oC8 > YD2 > YD30, which is consistent with the trend shown in the IPCE spectra. The inferior performance of YD30 is due to the limited ability of light harvesting through a lack of a diarylamino group in the *meso* position of the porphyrin ring. The values of V_{OC} of YD2-oC8 and YD30 were significantly greater than of V_{OC} of YD2 because of the effect of

Table 1. Photovoltaic Properties of Devices with YD2, YD2-oC8, and YD30 as Sensitizers on TiO₂ Thin Films (Thickness $\sim 3 \mu\text{m}$) under 1 sun Irradiation

porphyrins	J_{SC} (mA cm ⁻²)	V_{OC} (mV)	FF	η (%)
YD2	9.02	746	0.72	4.8
YD2-oC8	9.98	781	0.66	5.1
YD30	6.81	775	0.68	3.6

the long alkoxy chains attached at the *ortho* positions of the *meso*-phenyls.^{5,17} The overall photovoltaic performances of the thin-film samples are consistent with those of the optimized devices;⁵ the observed E-PL results measured for TiO₂ films of thickness $\sim 3 \mu\text{m}$ are utilized to rationalize the photovoltaic performances of porphyrin dyes in this series.

To test the effect of an electric field on emission spectra of porphyrins isolated in thin-film samples, YD2, YD2-oC8, or YD30 was embedded in PMMA films of thickness $\sim 0.5 \mu\text{m}$, and PL and E-PL were obtained with spectra on modulation of an electric field. Figure 2 shows the results at field strength 0.1

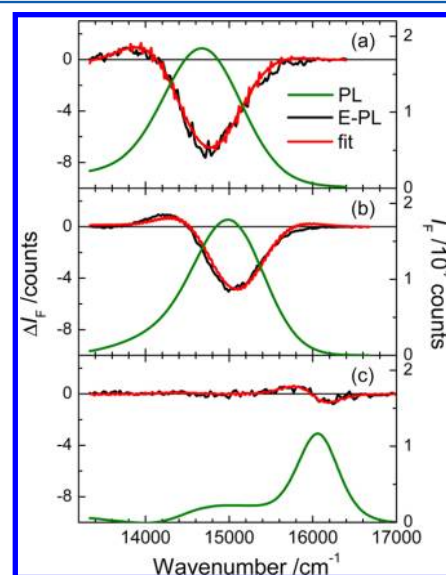


Figure 2. PL ($I_F(\bar{\nu})$, green traces) and E-PL ($\Delta I_F(\bar{\nu})$, black traces) spectra with field strength 0.1 MV cm⁻¹ for (a) YD2, (b) YD2-oC8, and (c) YD30 embedded in PMMA thin films. Red traces are simulated curves according to eq 2. Excitation wavelengths are (a) 441, (b) 464, and (c) 404 nm.

MV cm⁻¹. The E-PL spectra were reproduced with the zeroth, first, and second derivatives of the PL spectra in a linear combination, and those of each fit component are shown in Supporting Information Figure S2. The coefficients A , B , and C were evaluated according to eq 2, and the results are summarized in Table 2. The magnitudes of $\Delta\bar{\alpha}$ and $\Delta\mu$ between an emitting state and the ground state were derived from B and C , based on eq 3; these results are also shown in Table 2. All E-PL spectra exhibited a bathochromic shift with respect to their PL spectra, i.e., a positive value of B , because species in an excited state have larger polarizabilities than species in a ground state. We observed a quenching of the field-induced fluorescence of both YD2 and YD2-oC8, i.e., a negative value of A , which is attributed to a relaxation to a CS state that is nonfluorescent in nature.³² This model is consistent with our observation that for push–pull porphyrins such as YD2 and YD2-oC8 the nonfluorescent CS state was involved. We

Table 2. Fitted Coefficients A , B , and C of E-PL Spectra of Both Porphyrin/PMMA and Porphyrin/TiO₂ Systems Obtained According to Eq 2 and $\Delta\bar{\alpha}$ and $\Delta\mu$ Obtained with Eq 3^a

films	porphyrins	A (MV ⁻² cm ²)	B (MV ⁻² cm)	C (MV ⁻²)	$\Delta\bar{\alpha}^b$ (Å ³)	$\Delta\mu^b$ (D)
PMMA	YD2	-0.000 20	0.07	35	249.9	8.6
	YD2-oC8	-0.000 13	0.05	23	178.5	7.0
	YD30	0.000 002	0.02	2	71.4	2.1
TiO ₂	YD2	-0.007	4	800	14 280	41.3
	YD2-oC8	-0.012	9	2800	32 130	77.3
	YD30	0.003	3	300	10 710	25.3

^aErrors are regarded as $\pm 15\%$ in all values. ^b f is assumed to be unity.

noticed also that the fluorescence of YD2 ($A = -0.000\ 20$ MV⁻² cm²) was quenched more than that of YD2-oC8 ($A = -0.000\ 13$ MV⁻² cm²) in PMMA. The values of $\Delta\mu$ in Table 2 imply that the electric-dipole moment in the excited state is larger for YD2 than that for YD2-o-C8, resulting in a separation of charge for YD2 more facilitated than for YD2-o-C8 from the emitting state in PMMA.

In contrast with YD2 and YD2-o-C8, the fluorescence of YD30 in PMMA was slightly enhanced with F ($A \sim 2 \times 10^{-6}$ MV⁻² cm²). Electric field effects on nonradiative processes have been examined in many cases such as pyrene,²⁸ anthracene,³³ tetraphenylporphyrin,³⁴ and polymers.^{23,35} The observed enhancement of E-PL of YD30 in PMMA implies that the fluorescence quantum yield was larger under external field than that at zero field. Because the radiative rate coefficient is generally field independent,³⁶ the observed enhanced fluorescence quantum yield in YD30 must be related to the decreased rate coefficients of one or more nonradiative processes. We therefore infer that the external electric field might retard the intersystem crossing (ISC) $S_1 \rightarrow T_1$ of YD30. All E-PL spectra were recorded with excitation wavelengths at which the field-induced change in absorbance was negligible.

PL and E-PL spectra were recorded also for YD2, YD2-oC8, and YD30 sensitized on TiO₂ films. Figure 3 shows the results.

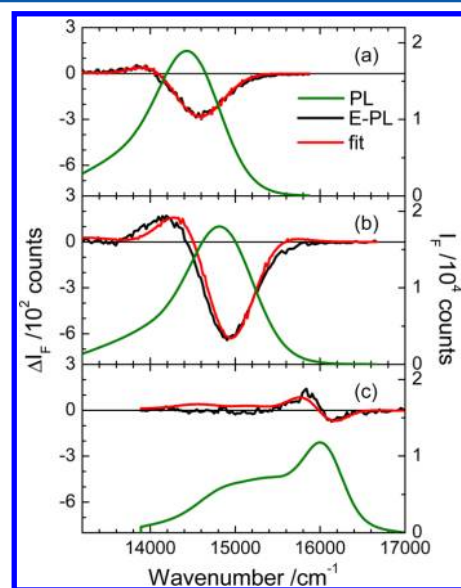


Figure 3. PL ($I_F(\bar{\nu})$, green traces) and E-PL ($\Delta I_F(\bar{\nu})$, black traces) spectra recorded with field strength 0.1 MV cm⁻¹ of (a) YD2, (b) YD2-oC8, and (c) YD30 adsorbed on TiO₂ thin films. Red traces are simulated curves according to eq 2. The excitation wavelengths are (a) 488, (b) 487, and (c) 400 nm.

The observed E-PL spectra were simulated satisfactorily with the zeroth, first, and second derivatives of the corresponding PL spectra in a linear combination (Supporting Information Figure S3); coefficients A , B , and C as well as $\Delta\bar{\alpha}$ and $\Delta\mu$ were evaluated, as in the case of the compounds in PMMA. The results are summarized in Table 2. Fluorescence spectra of these porphyrin/TiO₂ films are much red-shifted in the presence of F ; the value of B is much larger than that of porphyrin/PMMA counterparts. Both the large bathochromic spectral shift, i.e., larger polarizability in the excited state, and the large value of $\Delta\mu$ might be due to the porphyrins becoming anchored on the surface of TiO₂ in a deprotonated form.³⁷

As shown in Table 2, the coefficients (A , B , and C) are remarkably larger on TiO₂ films than the ones in PMMA films. These results indicate that the fluorescence of YD2 and YD2-oC8 adsorbed on TiO₂ films was quenched to a much greater extent than those in the PMMA films, likely because the character of charge separation of these push-pull porphyrins is much larger on TiO₂ films than in PMMA films. When the push-pull porphyrins adsorbed on TiO₂, the interfacial charge transfer character should also be considered. In this case, the distance of donor-acceptor (D-A) is longer than the molecular size, and the enhanced CS character may be attributed to the interfacial charge transfer from the dye to the TiO₂ surface. The absorption may correspond to the transition to the system's combined state with strong coupling between dye and TiO₂. That is the electron injection occurs following optical transition from the ground state of the dye to an excited state largely delocalized within the semiconductor (through the CS state), which was found to give rise to almost exactly the same absorption spectrum as for the dye in solution.³⁸

The photoinduced electrons of porphyrins in the excited state are considered to become rapidly injected into the conduction band (CB) of TiO₂ through the CS state of the porphyrins; this rapid injection led to efficient fluorescence quenching.^{15,25} The extents of fluorescence quenching and the changes of polarizability and electric dipole moments, both induced with an electric field, are greater for YD2-oC8 than for YD2 on TiO₂ films, indicating a stronger driving force to form the CS state in the former than in the latter. The *ortho*-substituted long alkoxy chains must play a key role to provide such a driving force for rapid formation of a CS state in YD2-oC8. In contrast with YD2 or YD2-o-C8, the fluorescence of YD30 sensitized on TiO₂ films was enhanced, indicating that electric fields retarded the ISC of YD30 both in PMMA films and on TiO₂ films. Nonradiative decay, including ISC, is considered to be suppressed by F to compete with electron injection at the emitting state of YD30. The extent of the enhancement on TiO₂ films was greater than that in PMMA

films, which might imply that the local field factor of the TiO₂ films is much larger than that of PMMA films.

We summarize in Figure 4 the fundamental photophysical and electron-transfer processes of the thin-film systems without

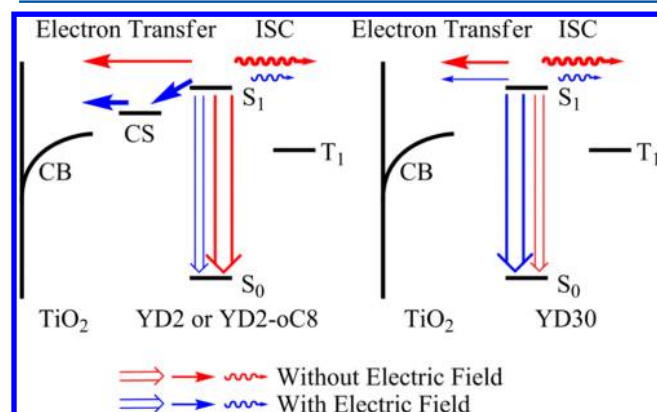


Figure 4. Schematic representation of fluorescence (double-solid-line arrows), electron transfer (solid-line arrows), and intersystem crossing (ISC) (multicurve arrows) of porphyrins of two types under conditions without (red) or with (blue) an applied external electric field.

(red) and with (blue) an applied electric field for porphyrins of two types. Three processes are indicated: multicurve arrows represent ISC, solid-line arrows the electron transfer, and double-solid-line arrows the radiative process. When we applied an electric field on porphyrins in PMMA films, we observed fluorescence quenching for porphyrins with an electron-donor substitute (YD2 or YD2-oC8) but fluorescence enhancement for a porphyrin without such a donor group (YD30). A nonfluorescent CS state is proposed to become involved in these two push–pull porphyrins so that the field-induced quenching of fluorescence was observed for both YD2 and YD2-oC8. In contrast, field-induced enhancement of fluorescence was observed for YD30 likely because the rate of ISC $S_1 \rightarrow T_1$ became diminished under a strong electric field. When those porphyrins were sensitized on TiO₂ films, an electron transfer from the S₁ state of porphyrin to the CB of TiO₂ became feasible. A further enhanced fluorescence of YD30 on TiO₂ indicates that nonradiative ISC and electron transfer in the YD30/TiO₂ system were significantly diminished under a large field. The involvement of the CS state in both YD2/TiO₂ and YD2-oC8/TiO₂ systems plays a key role to accelerate the rate of electron transfer through a consecutive process $S_1 \rightarrow CS \rightarrow CB$, so that the fluorescence became more quenched on the TiO₂ films than in the PMMA films. The extent of this field-induced quenching was more effective for YD2-oC8 than for YD2, indicating that the consecutive rate of electron transfer on the TiO₂ films was greater for the former than for the latter.

4. CONCLUSION

A field-induced quenching of fluorescence was observed for both push–pull porphyrins, YD2 and YD2-oC8, embedded in PMMA films or sensitized on TiO₂ films. For another porphyrin without an electron-donor group, YD30, the fluorescence was slightly enhanced on application of an electric field, likely because of the decreased nonradiative rates of ISC, under an applied electric field, which competes with electron injection into the CB of TiO₂. The involvement of a nonfluorescent CS state in both YD2 and YD2-oC8 thin-film

systems under a condition of a large field increases the rate of electron transfer from the excited state to the CS state that is responsible for the observed quenching of fluorescence. The extent of this quenching for the YD2-oC8/TiO₂ system was greater than that for the YD2/TiO₂ system, indicating that the *ortho*-substituted long alkoxy chains are the key components in YD2-oC8 to provide a driving force to accelerate the formation of a state of charge separation and the subsequent electron injection. Our results not only explain the photovoltaic performance for porphyrin sensitizers in this series but also evoke a new idea to accelerate the rate of electron transfer under an external electric field. Work is in progress to examine the effect of field-induced photovoltaic performance.

■ ASSOCIATED CONTENT

Supporting Information

Synthesis of YD30 and Figures S1–S3. This material is available free of charge via the Internet at <http://pubs.acs.org>.

■ AUTHOR INFORMATION

Corresponding Authors

*E-mail diau@mail.nctu.edu.tw (E.W.-G.D.).

*E-mail nohta@es.hokudai.ac.jp (N.O.).

*E-mail cyyeh@dragon.nchu.edu.tw (C.-Y.Y.).

Notes

The authors declare no competing financial interest.

■ ACKNOWLEDGMENTS

We thank Prof. Y.-P. Lee of NCTU for helpful discussions. National Science Council of Taiwan and Ministry of Education of Taiwan, under the ATU program, provided support for this project. Japan Science and Technology Agency (JST) also supported this project.

■ REFERENCES

- (1) Kamat, P. V.; Tvrdy, K.; Baker, D. R.; Radich, J. G. Beyond Photovoltaics: Semiconductor Nanoarchitectures for Liquid-Junction Solar Cells. *Chem. Rev.* **2010**, *110*, 6664–6688.
- (2) Martinez-Diaz, M. V.; de la Torre, G.; Torres, T. Lighting Porphyrins and Phthalocyanines for Molecular Photovoltaics. *Chem. Commun.* **2010**, *46*, 7090–7108.
- (3) Hagfeldt, A.; Boschloo, G.; Sun, L.; Kloo, L.; Pettersson, H. Dye-Sensitized Solar Cells. *Chem. Rev.* **2010**, *110*, 6595–6663.
- (4) Ning, Z.; Fu, Y.; Tian, H. Improvement of Dye-Sensitized Solar Cells: What We Know and What We Need to Know. *Energy Environ. Sci.* **2010**, *3*, 1170–1181.
- (5) Li, L. L.; Diau, E. W. G. Porphyrin-Sensitized Solar Cells. *Chem. Soc. Rev.* **2013**, *42*, 291–304.
- (6) Vougioukalakis, G. C.; Philippopoulos, A.; Stergiopoulos, T.; Falaras, P. Contributions to the Development of Ruthenium-based Sensitizers for Dye-Sensitized Solar Cells. *Coord. Chem. Rev.* **2011**, *255*, 2602–2621.
- (7) Yella, A.; Lee, H. W.; Tsao, H. N.; Yi, C.; Chandiran, A. K.; Nazeeruddin, M. K.; Diau, E. W. G.; Yeh, C. Y.; Zakeeruddin, S. M.; Grätzel, M. Porphyrin-Sensitized Solar Cells with Cobalt (II/III)-Based Redox Electrolyte Exceed 12% Efficiency. *Science* **2011**, *334*, 629–634.
- (8) Wang, Q.; Ito, S.; Grätzel, M.; Fabregat-Santiago, F.; Mora-Seró, I.; Bisquert, J.; Bessho, T.; Imai, H. Characteristics of High Efficiency Dye-Sensitized Solar Cells. *J. Phys. Chem. B* **2006**, *110*, 25210–25221.
- (9) Yu, Q.; Wang, Y.; Yi, Z.; Zu, N.; Zhang, J.; Zhang, M.; Wang, P. Highly Efficient Dye-Sensitized Solar Cells: The Influence of Lithium Ions On Exciton Dissociation, Charge Recombination, and Surface States. *ACS Nano* **2010**, *4*, 6032–6038.

- (10) Zhang, G.; Bala, H.; Cheng, Y.; Shi, D.; Lv, X.; Yu, Q.; Wang, P. High Efficiency and Stable Dye-Sensitized Solar Cells with an Organic Chromophore Featuring a Binary π -Conjugated Spacer. *Chem. Commun.* **2009**, 2198–2100.
- (11) Zeng, W.; Cao, Y.; Bai, Y.; Wang, Y.; Shi, Y.; Zhang, M.; Wang, F.; Pan, C.; Wang, P. Efficient Dye-Sensitized Solar Cells with an Organic Photosensitizer Featuring Orderly Conjugated Ethylenedioxythiophene and Dithienosilole Blocks. *Chem. Mater.* **2010**, *22*, 1915–1925.
- (12) Maiti, N. C.; Mazumdar, S.; Periasamy, N. J- and H-Aggregates of Porphyrin-Surfactant Complexes: Time-Resolved Fluorescence and Other Spectroscopic Studies. *J. Phys. Chem. B* **1998**, *102*, 1528–1538.
- (13) Aggarwal, L. P. F.; Borissevitch, I. E. On the Dynamics of the TPPS₄ Aggregation in Aqueous Solutions Successive Formation of H and J Aggregates. *Spectrochim. Acta, Part A* **2006**, *63*, 227–233.
- (14) Lee, C. W.; Lu, H. P.; Lan, C. M.; Huang, Y. L.; Liang, Y. R.; Yen, W. N.; Liu, Y. C.; Lin, Y. S.; Diao, E. W. G.; Yeh, C. Y. Novel Zinc Porphyrin Sensitizers for Dye-Sensitized Solar Cells: Synthesis and Spectral, Electrochemical, and Photovoltaic Properties. *Chem.—Eur. J.* **2009**, *15*, 1403–1412.
- (15) Lu, H. P.; Tsai, C. Y.; Yen, W. N.; Hsieh, C. P.; Lee, C. W.; Yeh, C. Y.; Diao, E. W. G. Control of Dye Aggregation and Electron Injection for Highly Efficient Porphyrin Sensitizers Adsorbed on Semiconductor Films with Varying Ratios of Coadsorbate. *J. Phys. Chem. C* **2009**, *113*, 20990–20997.
- (16) Bessho, T.; Zakeeruddin, S. M.; Yeh, C. Y.; Diao, E. W. G.; Grätzel, M. Highly Efficient Mesoscopic Dye-Sensitized Solar Cells Based on Donor-Acceptor Substituted Porphyrins. *Angew. Chem., Int. Ed.* **2010**, *49*, 6646–6649.
- (17) Chang, Y. C.; Wang, C. L.; Pan, T. Y.; Hong, S. H.; Lan, C. M.; Kuo, H. H.; Lo, C. F.; Hsu, H. Y.; Lin, C. Y.; Diao, E. W. G. A Strategy to Design Highly Efficient Porphyrin Sensitizers for Dye-Sensitized Solar Cells. *Chem. Commun.* **2011**, *47*, 8910–8912.
- (18) Wang, C. L.; Lan, C. M.; Hong, S. H.; Wang, Y. F.; Pan, T. Y.; Chang, C. W.; Kuo, H. H.; Kuo, M. Y.; Diao, E. W. G.; Lin, C. Y. Enveloping Porphyrins for Efficient Dye-Sensitized Solar Cells. *Energy Environ. Sci.* **2012**, *5*, 6933–6940.
- (19) Zdyb, A.; Krawczyk, S. Molecule-Solid Interaction: Electronic States of Anthracene-9-carboxylic Acid Adsorbed on the Surface of TiO₂. *Appl. Surf. Sci.* **2010**, *256*, 4854–4858.
- (20) Krawczyk, S.; Zdyb, A. Electronic Excited States of Carotenoid Dyes Adsorbed on TiO₂. *J. Phys. Chem. C* **2011**, *115*, 22328–22335.
- (21) Jalviste, E.; Ohta, N. Stark Absorption Spectroscopy of Indole and 3-Methylindole. *J. Chem. Phys.* **2004**, *121*, 4730–4739.
- (22) Mehata, M. S.; Iimori, T.; Yoshizawa, T.; Ohta, N. Electroabsorption Spectroscopy of 6-Hydroxyquinoline Doped in Polymer Films: Stark Shifts and Orientational Effects. *J. Phys. Chem. A* **2006**, *110*, 10985–10991.
- (23) Mehata, M. S.; Hsu, C. S.; Lee, Y. P.; Ohta, N. Electric Field Effects on Photoluminescence of Polyfluorene Thin Films: Dependence on Excitation Wavelength, Field Strength, and Temperature. *J. Phys. Chem. C* **2009**, *113*, 11907–11915.
- (24) Ardo, S.; Sun, Y.; Castellano, F. N.; Meyer, G. J. Excited-State Electron Transfer from Ruthenium-Polypyridyl Compounds to Anatase TiO₂ Nanocrystallites: Evidence for a Stark Effect. *J. Phys. Chem. B* **2010**, *114*, 14596–14604.
- (25) Pastore, M.; De Angelis, F. Computational Modeling of Stark Effects in Organic Dye-Sensitized TiO₂ Heterointerfaces. *J. Phys. Chem. Lett.* **2011**, *2*, 1261–1267.
- (26) Cappel, U. B.; Feldt, S. M.; Schöneboom, J.; Hagfeldt, A.; Boschloo, G. The Influence of Local Electric Fields on Photoinduced Absorption in Dye-Sensitized Solar Cells. *J. Am. Chem. Soc.* **2010**, *132*, 9096–9101.
- (27) Ito, S.; Chen, P.; Comte, P.; Nazeeruddin, M. K.; Liska, P.; Péchy, P.; Grätzel, M. Fabrication of Screen-Printing Pastes from TiO₂ Powders for Dye-Sensitized Solar Cells. *Prog. Photovoltaics* **2007**, *15*, 603–612.
- (28) Umeuchi, S.; Nishimura, Y.; Yamazaki, I.; Murakami, H.; Yamashita, M.; Ohta, N. Electric Field Effects on Absorption and Fluorescence Spectra of Pyrene Doped in a PMMA Polymer Film. *Thin Solid Films* **1997**, *311*, 239–245.
- (29) Luo, L. Y.; Lo, C. F.; Lin, C. Y.; Chang, I. J.; Diao, E. W. G. Femtosecond Fluorescence Dynamics of Porphyrin in Solution and Solid Films: The Effects of Aggregation and Interfacial Electron Transfer between Porphyrin and TiO₂. *J. Phys. Chem. B* **2006**, *110*, 410–419.
- (30) Jalviste, E.; Ohta, N. Theoretical Foundation of Electroabsorption Spectroscopy: Self-Contained Derivation of the Basic Equations with the Direction Cosine Method and the Euler Angle Method. *J. Photochem. Photobiol., C* **2007**, *8*, 30–46.
- (31) Ohta, N. Electric Field Effects on Photochemical Dynamics in Solid Films. *Bull. Chem. Soc. Jpn.* **2002**, *75*, 1637–1655.
- (32) Kubo, M.; Mori, Y.; Otani, M.; Murakami, M.; Ishibashi, Y.; Yasuda, M.; Hosomizu, K.; Miyasaka, H.; Imahori, H.; Nakashima, S. Ultrafast Photoinduced Electron Transfer in Directly Linked Porphyrin-Ferrocene Dyads. *J. Phys. Chem. A* **2007**, *111*, 5136–5143.
- (33) Nakabayashi, T.; Wu, B.; Morikawa, T.; Iimori, T.; Rubin, M. B.; Speiser, S.; Ohta, N. External Electric Field Effects on Absorption and Fluorescence of Anthracene-(CH₂)_n-Naphthalene Bichromophoric Molecules Doped in a Polymer Film. *J. Photochem. Photobiol., A* **2006**, *178*, 236–241.
- (34) Iwaki, Y.; Ohta, N. Electric-Field-Induced Quenching of Fluorescence of Tetraphenylporphyrin in a PMMA Polymer Film. *Chem. Lett.* **2000**, 894–895.
- (35) Mehata, M. S.; Hsu, C. S.; Lee, Y. P.; Ohta, N. Electroabsorption and Electrophotoluminescence of Poly(2,3-diphenyl-5-hexyl-p-phenylene vinylene). *J. Phys. Chem. C* **2012**, *116*, 14789–14795.
- (36) Lockhart, D. J.; Hammes, S. L.; Franzen, S.; Boxer, S. G. Electric Field Effects on Emission Line Shapes When Electron Transfer Competes with Emission: An Example from Photosynthetic Reaction Centers. *J. Phys. Chem.* **1991**, *95*, 2217–2226.
- (37) Pérez León, C.; Kador, L.; Peng, B.; Thelakkat, M. Characterization of the Adsorption of Ru-bpy Dyes on Mesoporous TiO₂ Films with UV-Vis, Raman, and FTIR Spectra. *J. Phys. Chem. B* **2006**, *110*, 8723–8730.
- (38) De Angelis, F.; Fantacci, S.; Mosconi, E.; Nazeeruddin, M. K.; Grätzel, M. Absorption Spectra and Excited State Energy Levels of the N719 Dye on TiO₂ in Dye-Sensitized Solar Cell Models. *J. Phys. Chem. C* **2011**, *115*, 8825–8831.